论文	作者
Statistical Correlation Analysis Between Thermal Infrared Anomalies Observed From MTSATs and Large Earthquakes Occurred in Japan (2005–2015)	N. Genzano and V. Tramutoli

> 本文作者提供的其他不同的研究状况，供参考。

Table 1
Long-Term Statistical Analysis Carried Out Within Different Studies

Parameter	TEMPORAL coverage	STUDIED region	Earthquake magnitude	Reference
Plasma frequency at the ionospheric F2 peak foF2	1994–1999	Taiwan	$M \geq 5$	Liu et al. (2006)
Ionospheric ion density recorded by DEMETER[a]	2004–2010	World	$M \geq 4.8$	M. Li and Parrot (2013)
Ionospheric electron density derived from GIM-TEC map	2000–2010	World	$M \geq 6$	Le et al. (2011)
	1998–2010	Japan	$M \geq 6$	Kon et al. (2011)
	2003–2012	World	$M \geq 7$	Zhu et al. (2014)
	1998–2014		$M \geq 5$	Shah and Jin (2015)
	2000–2013	China	$M \geq 5$	Ke et al. (2016)
	2000–2014	World	$M \geq 6$	Thomas et al. (2017)
	2003–2014		$M \geq 6$	Zhu et al. (2018)
TEC derived from ground-based GPS receivers	2001–2007	Taiwan	$M \geq 5$	Liu et al. (2010)
Subionospheric VLF/LF perturbations	2001–2007	Japan	$M \geq 6$	Hayakawa et al. (2010)
Atmospheric lights and luminous phenomena	1993–2004	Taiwan	$M \geq 5$	Liu et al. (2015)
Earth's outgoing longwave radiation	2009–2019	Taiwan	$M \geq 6$	Fu et al. (2020)
Earth's thermally emitted radiation	2004–2013	Greece	$M \geq 4$	Elefteriou et al. (2016)
	2002–2018	Sichuan (China)		Zhang and Meng (2019)
	2004–2014	Italy		Genzano et al. (2020)
ULF geomagnetic fields	2001–2010	Central Japan	$M \geq 4$	Han et al. (2014, 2017, 2020); Hattori et al. (2013)
ECMWF climatological reanalysis data	1994–2016	Central Italy	$M \geq 5$	Piscini et al. (2017)
GPS measurements of ground deformation	2004–2008	North Island, New Zealand	$M \geq 5.1$	T. Wang et al. (2013)
	1999–2009	Southern California	$M \geq 4.7$	
	1997–2010	Central Japan	$M \geq 5.5$	

1.数据和方法

通过分析**MTSAT-1R**卫星上的JAMI传感器在2005年6月至2010年6月期间以及**MTSAT-2**卫星上的IMAGER传感器在2010年7月至2015年12月期间以10.8微米（10.3-11.3微米）获取的所有夜间（00:30 LT；即15:30 UTC-1天）TIR图像，确定了热异常。这些图像属于千叶大学CEReS提供的空间分辨率为0.04°的网格化数据集。

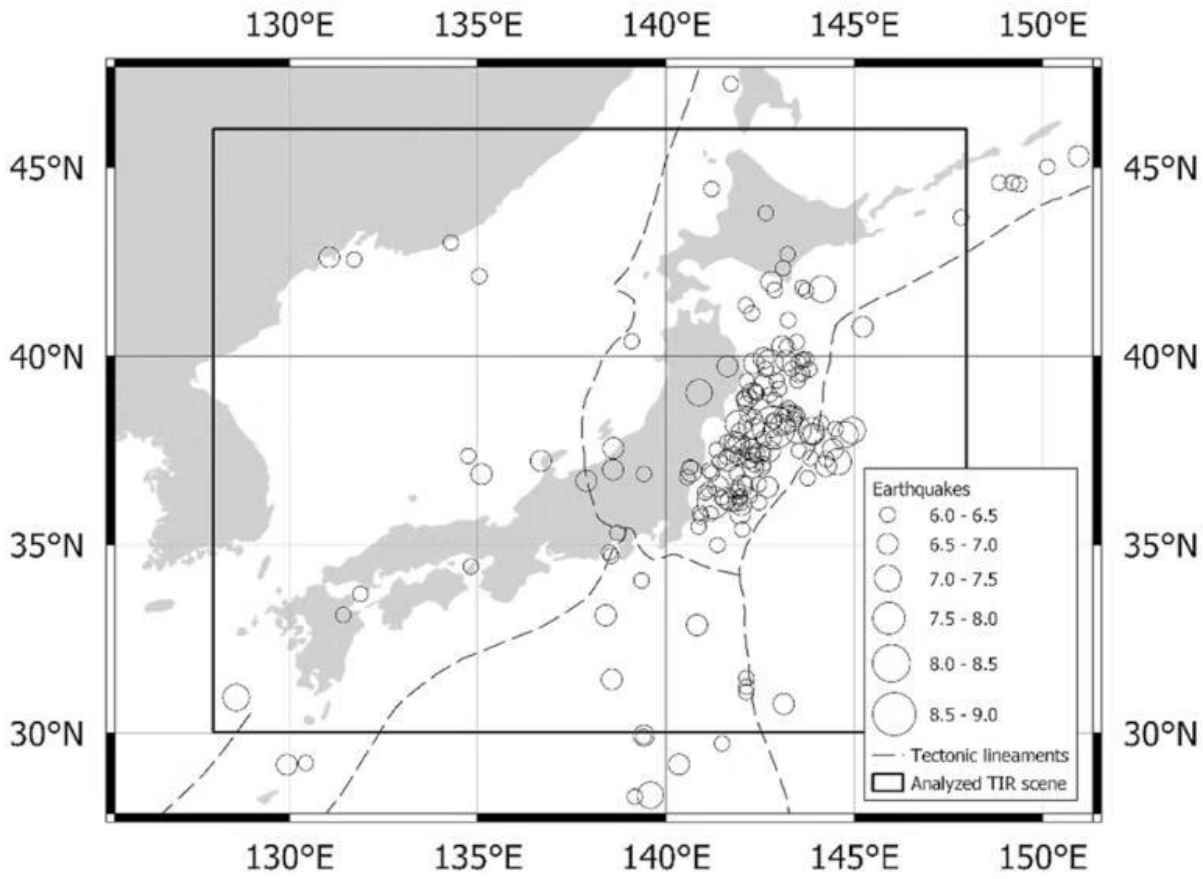

Figure 1. Investigated area. The rectangular black solid line contains the area of the analyzed MTSAT TIR scene; circles indicate earthquakes with $M_{JMA} \geq 6$ occurred from June 15, 2005, to January 31, 2016, inside the wider area 27°N–49°N and 125°E–151°E.

> 图1显示了调查区域（北纬30-46°，东经128-148°），该区域涵盖了日本领土。这里还显示了2005年6月15日至2016年1月31日期间发生在比调查区域大3°的地区的地震。根据日本气象厅的地震目录（日本气象厅，2021年），有229个MJMA≥6的事件和79个MJMA≥6.5的事件，发生在所考虑的时间段和选定的地理区域。

在这项研究中，为了识别TIR异常，使用了基于统计学的TIR异常估计器（RETIRA；Filizzola等人，2004；Tramutoli等人，2005）指数，在Genzano等人（2020）称为RETIRAbox

$$\otimes_{\Delta T_{box}}(x,y,t) \equiv \frac{\Delta T_{box}(x,y,t) - \mu_{\Delta T_{box}}(x,y)}{\sigma_{\Delta T_{box}}(x,y)} \quad (1)$$

where

- (x, y) are the geographical coordinates corresponding to the center of the pixel.
- t is the satellite acquisition time with $t \in \tau$, being τ the temporal domain including all the nighttime MT-SAT images collected at 00:30 LT from June 2005 to December 2015.
- $\Delta T_{box}(x,y,t)$ is the spatial average of $\Delta T(x,y,t)$ within a region of 3 × 3 pixels centered at location (x,y). Its computation takes place only if at least 55% of pixels within the box are clear and not close to clouds (cloud-free boxes). The One-channel Cloudy-radiance-detection Approach (OCA; Cuomo et al., 2004) algorithm identified cloudy pixels.
- $\Delta T(x,y,t) = T(x,y,t) - T(t)$ is the difference between the punctual values of the TIR brightness temperature $T(x,y,t)$ and the daily spatial average $T(t)$. It should be stressed that $T(t)$ computation takes account only of cloud-free values of the whole investigated region, which is part of the identical category (i.e., only sea or land pixels if (x,y) is on the sea or land, respectively).
- $\mu_{\Delta T_{box}}(x,y)$ and $\sigma_{\Delta T_{box}}(x,y)$ are the values of time average and standard deviation of $\Delta T_{box}(x,y,t)$ reckoned on cloud-free boxes belonging to the chosen data set ($t \in \tau$).

作者在这里采用了Eleftheriou等人（2016）提出的改进的RST预处理阶段，以减少气象云对参考场计算可能产生的负面影响以及随之而来的可能的假阳性的扩散。事实上，在日本这样的地理环境中，这种影响可能特别大，因为在一个相对较小的土地范围内，受到各种气候条件的影响。此外，它还受到一些现象的影响，如夏季和初秋时南部的季风，8月至10月太平洋一侧的台风，以及日本海北部鄂霍次克海大气压力的影响。

So, for each month of the year, we computed two images ($\mu_{\Delta T_{box}}$ and $\sigma_{\Delta T_{box}}$ images) used as "reference images" (i.e., RST reference fields) for the calculation of the $RETIRA_{box}$ index. They are representative of the expected thermal conditions.

Using such reference fields, we calculated *Thermal Anomaly Maps* (TAMs) for all MTSAT-1R/2 TIR images (i.e., 3,747 in the period June 2005 to December 2015); TAMs report the value of $\otimes_{\Delta T_{box}}(x,y,t)$ for all cloud-free locations. From now on, we consider as *Thermal Anomalies* (TAs) those locations with $\otimes_{\Delta T_{box}}(x,y,t) \geq 3.5$—that is, with signal excess $\Delta T_{box}(x,y,t) - \mu_{\Delta T_{box}}(x,y) \geq 3.5\,\sigma_{\Delta T_{box}}(x,y)$.

Significant Sequence of Thermal Anomalies (SSTAs)需满足以下条件：

- *Relative intensity*. TAs should have a value of $\otimes_{\Delta T_{box}}(x,y,t) \geq K$ (in this paper, $K = 3.5$).
- *Discard of spurious effects*. Portions of the scene (i.e., land or sea) of the TAMs with a large cloud cover, navigation errors (Filizzola et al., 2004), and known spurious effects (see Aliano, Corrado, Filizzola, Genzano, et al., 2008; Eleftheriou et al., 2016; Genzano et al., 2009, 2015 for more details) are discarded from the subsequent analyses; about cloud cover, in this study, we consider useful only portions of the scene having a fraction of cloudy pixels less than 80% of those belonging to the same land/sea class.
- *Minimum spatial extension*. Each STA has to cover at least an area of 150 km^2 within a region of 1° × 1° around (x,y).
- *Persistence in space–time domain*. STAs are 1° distant maximum from each other (spatial persistence) and reappear at least another time in the 7 days preceding/following t (temporal persistence).

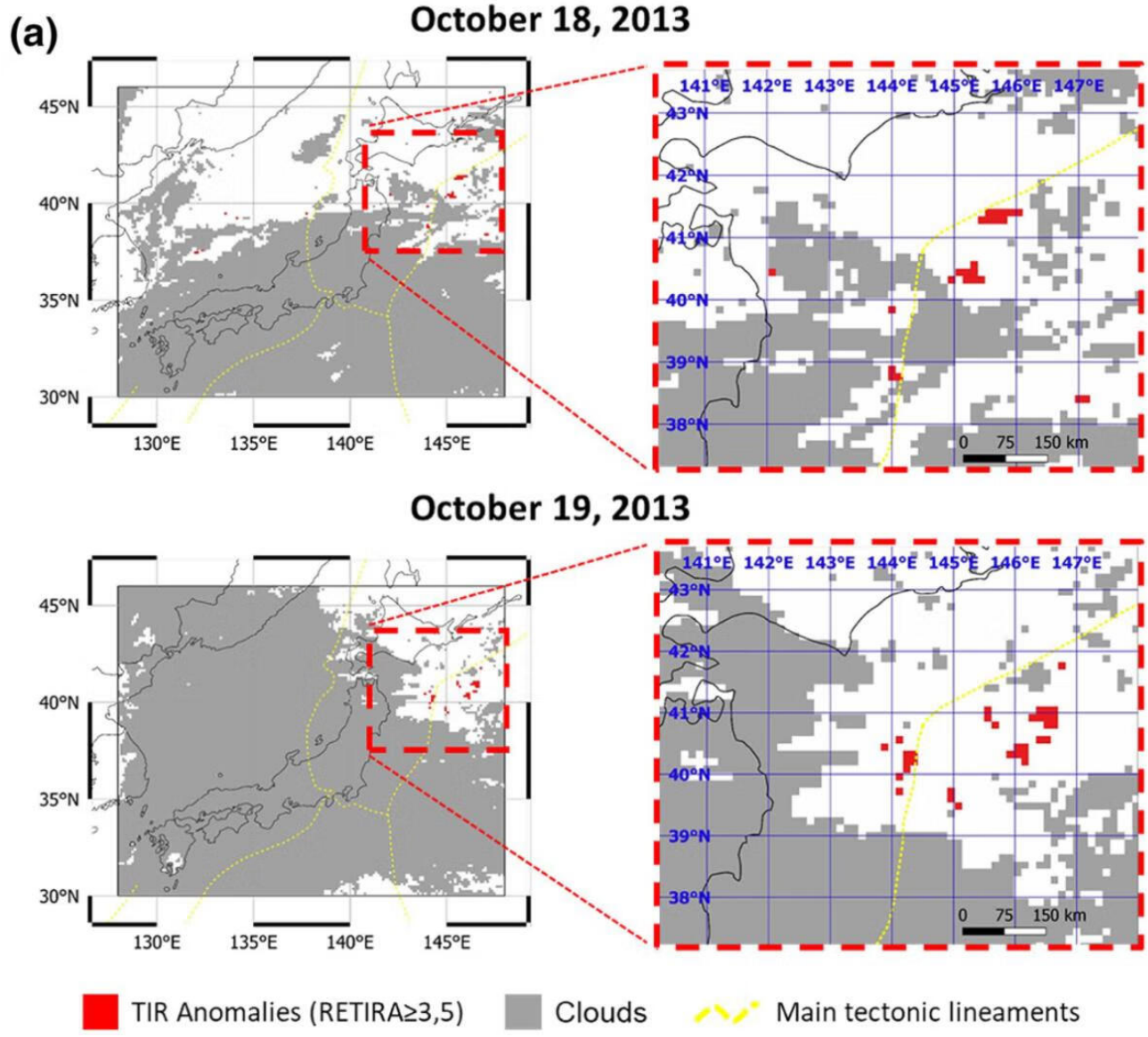
(a)
October 18, 2013
45°N
40°N
35°N
30°N
130°E
135°E
140°E
145°E
141°E 142°E 143°E 144°E 145°E 146°E 147°E
43°N
42°N
41°N
40°N
39°N
38°N
0 75 150 km
October 19, 2013
TIR Anomalies (RETIRA≥3,5)
Clouds
Main tectonic lineaments

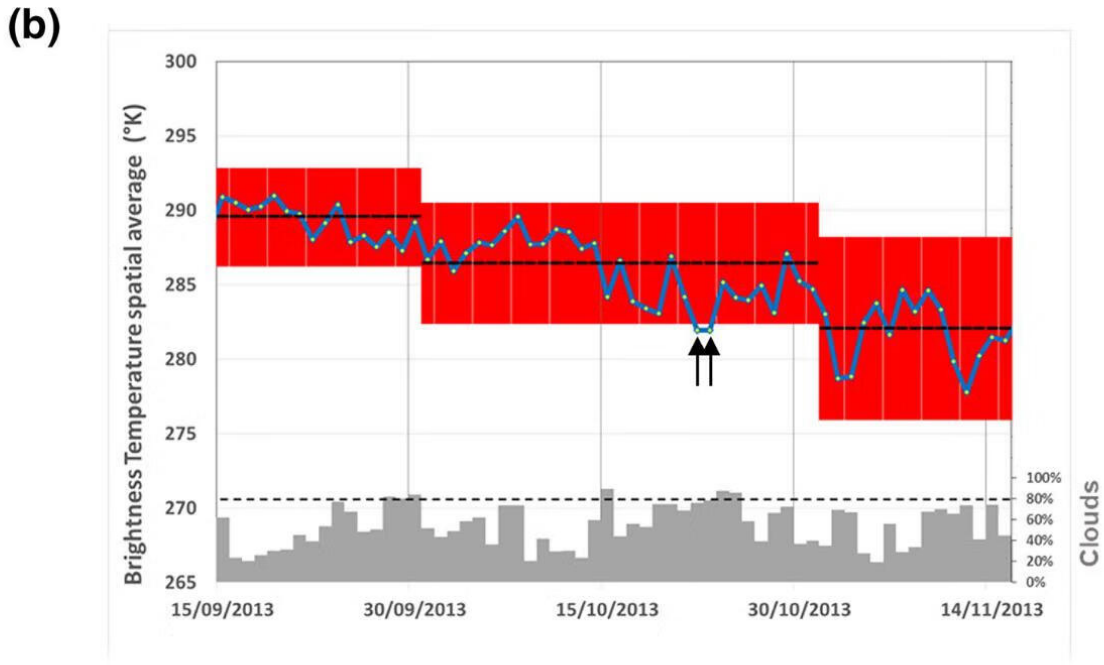

Figure 2. (a) TAMs where STAs appear with an appreciable extension (i.e., at least 150 km^2) and a space–time persistence on October 18 and 19, 2013, over the Pacific Sea. (b) The analysis was necessary to identify TAs due to meteorological effects. The yellow circles indicate the daily spatial averages $T(t)$ over sea computed on cloud-free pixels; the black lines indicate the temporal averages (μ_T); the red zone defines the $\pm 2\ \sigma_T$ bounds used for excluding images affected by the *cold spatial average effect* (like the ones indicated by the black arrows), which have been computed by using all images available in the period 2005–2015 during the same month; the gray bars represent the cloud percentage over the sea part of the scene. TAMs, Thermal Anomaly Maps; STAs, Significant Thermal Anomalies; TAs, Thermal Anomalies.

2.数据分析

2.1地震目录过滤

> 地震集群可能对结果有影响,地震目录的解聚是一个基本的初步分析，其质量可能影响后续分析的结果。

在这项研究中，采用了特定的标准来选择相关分析中考虑的地震。由于相邻地区在一个时间跨度ts中可能发生不止一次地震，对于在ts中发生的每个地震事件：

（a）我们计算了相应的Dobrovolsky半径（Dobrovolsky等人，1979），其中Mi是第i次地震的震级； （b）我们按照震级的大小和发生时间的递增进行排序； （c）从列表中的第一个震例开始，我们排除了所有落在其Dobrovolsky半径内的震例； （d）我们对列表中所有幸存的震例重复这个过程，直到所有的震例都被评估过。

对于这项研究，我们生成了两个不同的过滤目录：

- Daily filtered catalog, where ts = 1 day. We used this catalog for a preliminary evaluation of comparative performance between the traditional RST analysis and its optimized arrangement, here presented. This filtered catalog consists of 157 events with MJMA ≥ 6 and 58 events with MJMA ≥ 6.5.
- Monthly filtered catalog, where ts = ±30 days. We used this catalog to evaluate if the high seismicity of the Japanese region could affect results concerning the RST-optimized arrangement. This filtered catalog consists of 82 events with MJMA ≥ 6 and 35 events with MJMA ≥ 6.5.

2.2基于RST的TIR异常与地震（MJMA≥6）发生的相关性分析

我们将上述规则应用于2005年6月至2015年12月期间的所有MTSAT TIR图像，并确定了60个SSTA（分布在132个不同的TIR图像上，即占所有可用TIR图像的3.5%）。

我们评估了SSTA的出现与属于每日过滤目录的地震的位置、时间和震级之间可能的相关性。为此，我们应用了经验规则，这些规则是在考虑到以前的研究（见Tramutoli, Corrado, Filizzola, Genzano, Lisi, & Pergola, 2015; Tramutoli et al., 2018, and references therein）和迄今为止提出的解释大地震前后TA出现的物理模型（如Tramutoli et al., 2013）后建立的。此外，定义的验证规则，应驱动回顾性的相关分析，与CSEP项目（Schorlemmer等人，2018）使用的规则相匹配。

按照这样的规则，我们认为在一个地理位置（x,y）上观察到的每一个STA，在时间t，并且属于先前确定的SSTA，与M≥6的地震事件相关，如果它发生在规定的范围内：

- 时间窗口，即在（震前异常）最后一次出现TA后30天内，或直到（震后/地震异常）第一次出现TA前15天内。
- 空间窗口，即与形成SSTA的TA的距离RD内，其中RD=10^0.43M，即Dobrovolsky半径（Dobrovolsky等人，1979）。

图3显示了应用规则的示意图。对于2013年10月18-19日的SSTA，为验证TA和地震事件之间的可能关系，对不同级别的地震震级定义了一个时空体积（这里只有M≥6和6.5的地震用不同颜色表示）。满足上述定义的地震为红点。在这种情况下，2013年10月18日和19日在日本东北海岸出现的STA，之后发生了一次7.1级的地震。它发生在太平洋上第一次出现的TA之后8天（即2013年10月26日）。

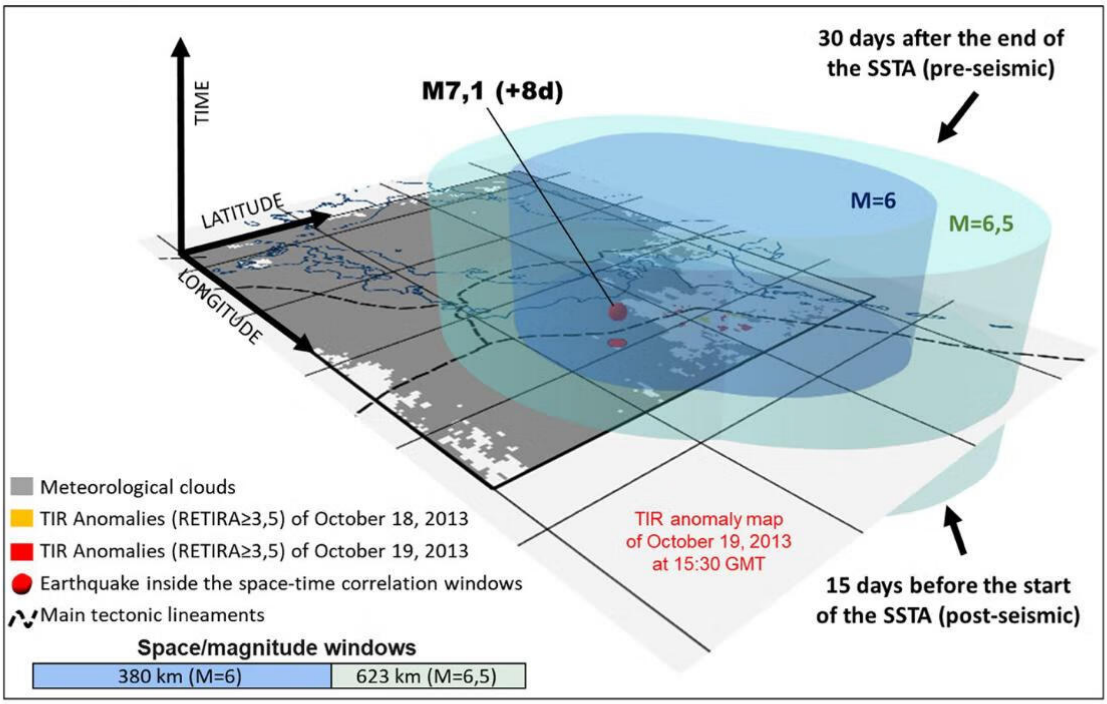

Figure 3. A schematic view of the applied correlation rules. The colored cylinders around the identified SSTA (October 18 and 19, 2013) represent the alerted space–time volumes for different classes of earthquake magnitude (see text for more details). In addition to STAs of October 19 (represented by red pixels), STAs of October 18 (represented by orange pixels) are superimposed to the TIR anomaly map of October 19, 2013, as well. The red ball (with its projection on the map) represents the earthquake inside the correlation rules, and the label indicates its magnitude and temporal distance (in days) from the first STA appearance (i.e., October 18, 2013). SSTA, Significant Sequence of Thermal Anomaly; STAs, Significant Thermal Anomalies; TIR, Thermal InfraRed.

2.3减少假阳性TIR异常的发生

在本文中，我们提出了一个不同的标准来计算RST参考场。我们没有使用FWC（fixed-monthly window criterion），**而是在一年中每个被分析的日子周围使用了30天的时间窗口（即±15天）**（移动窗口标准，MWC）来建立（366×2而不是12×2）参考场。通过这种方式，我们计算了732幅参考场图像（一年中的每一天都有两幅，μ和σ，图像），而不是24幅月度参考场图像（一年中的每个月都有两幅，μ和σ，图像）。这使我们能够将TIR记录与最合适的参考场进行比较。在一年中的某些地理区域和时期，这种选择可以大大减少发生在月初/月末的热异常现象的扩散。沿着上述步骤，我们对SSTA和属于每日过滤目录的地震进行了新的相关分析。使用以前用于评估RSTFWC性能的相同目录，使我们能够更好地判断RSTMWC与RSTFWC相比所取得的改进。

这项新的分析强调，在2005年6月至2015年12月期间，在日本地区的29个确定的SSTA（在这种情况下，分布在69个不同的TIR图像上，即占全部可用TIR图像的1.8%）中，有62.1%显然在空间和时间上与报告的地震事件有关（MJMA≥6）。

比较两个独立的 RST 分析，应关注以下方面的减少：

- the number of SSTAs from 60 (highlighted by using the traditional RST analysis, RST_{FWC}) to 29 (highlighted by using the proposed innovative RST analysis, RST_{MWC});
- the false-positive SSTAs from 30 (corresponding to 50% of all SSTAs) to only 11 (corresponding to 37.9% of all SSTAs).

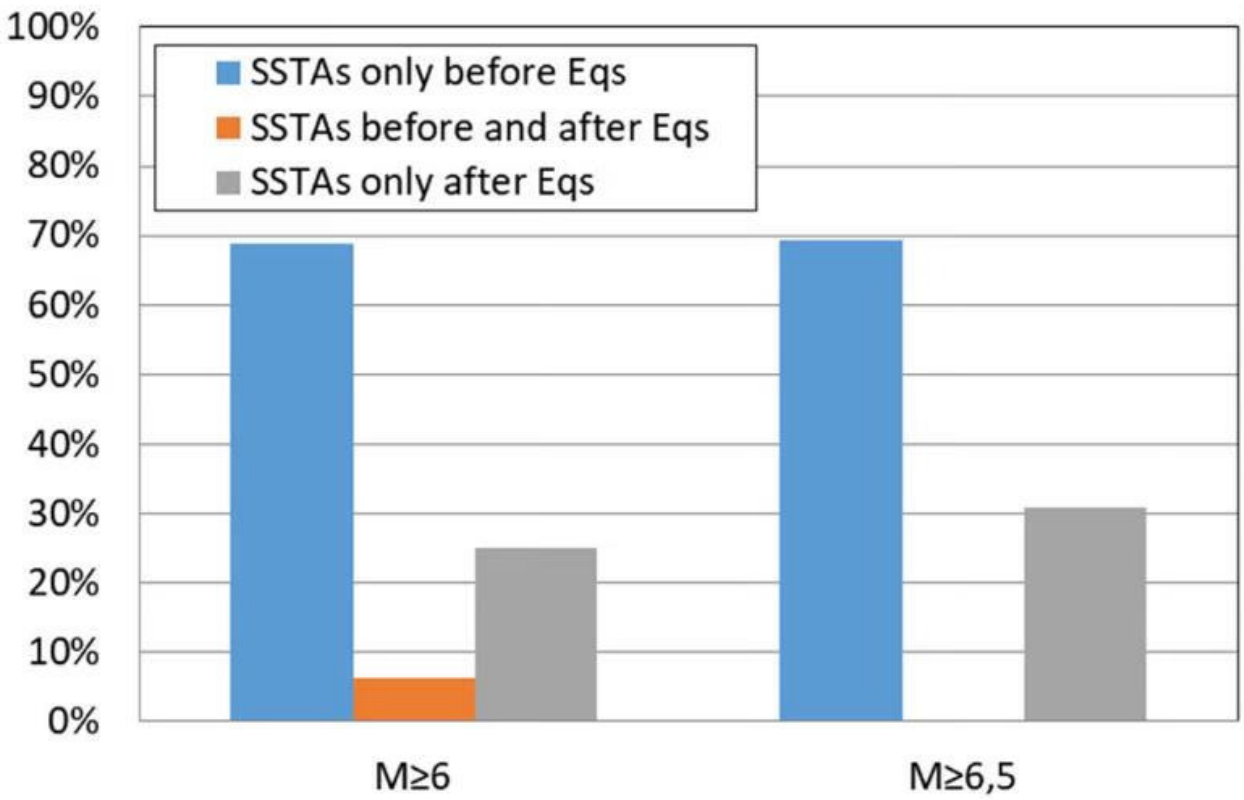

Figure 4. The RST_{MWC}-based SSTA distribution compared to the occurrences of seismic events of magnitude 6 and 6.5. SSTA, Significant Sequence of Thermal Anomaly.

震前SSTA占主导地位

我们进行了随机测试分析，目的是评估所取得的结果的质量和 "基于RST的卫星热异常 "参数对专门用于评估短期地震危险的多参数系统的潜在信息贡献。这种分析还应该强调，如果SSTA（包括事件前和事件后）看起来与

地震有关，只是因为所研究地区的高地震率和/或因为使用的相关空间/时间规则（最终设置得太大）。

我们考虑了**Molchan**方法（Molchan，1997年，以及其中的参考文献），作为验证基于SSTA的实际值的参考方法，与基于随机的报警函数相比。

根据所调查参数的具体特征（即基于 RST 的 SSTA）采用 Shebalin 等人提出的定制 Molchan 误差图。（2006），而不是使用基于似然检验的方法。

$$\nu_{\mathrm{EQ}}(M) = \frac{\text{number of EQs with magnitude} \geq M \text{ outside the space–time correlation window (missed)}}{\text{total number of EQs with magnitude} \geq M \text{ occurred within the whole space} \times \text{time volume}} \quad (2)$$

$$\tau_{\mathrm{SSTA}}(M) = \frac{\text{alerted space} \times \text{time volume for EQs with magnitude} \geq M}{\text{whole investigated space} \times \text{time volume}} \quad (3)$$

同时，作者还计算了概率增益（Aki，1989）G=（1-νEQ）/τSSTA，以及基于无效假设的置信极限曲线（详见Kossobokov，2006），在随机猜测的对角线周围95%的水平。

误差图结果如下图。

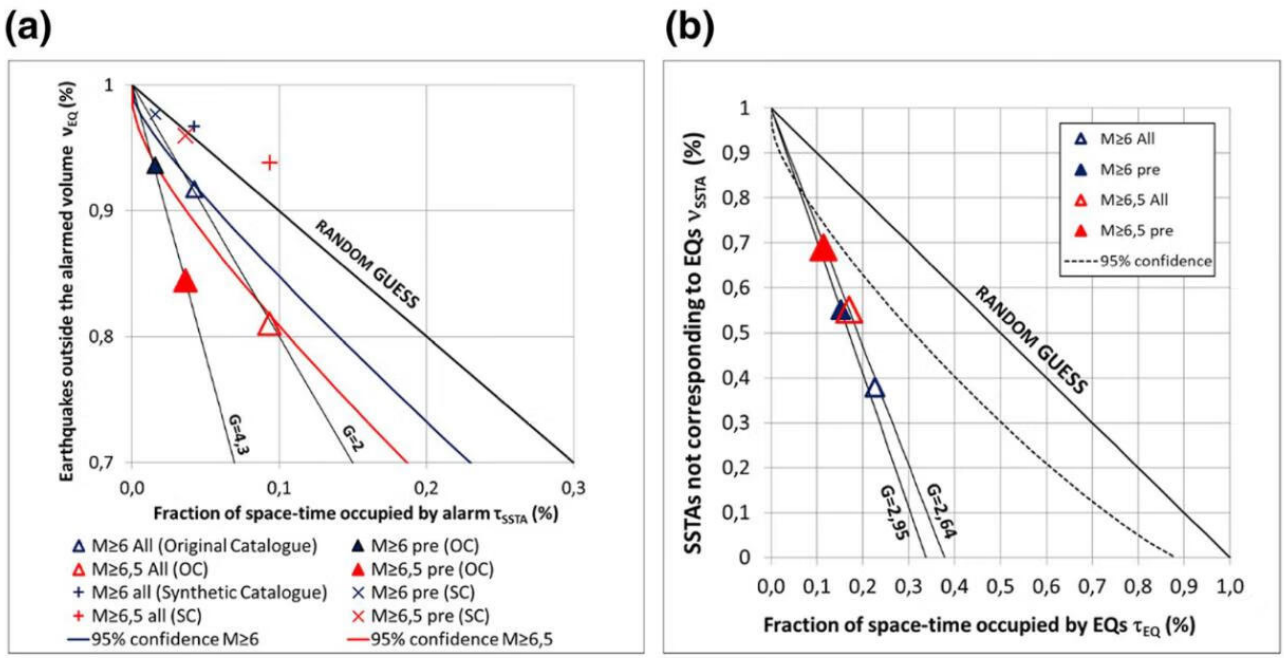

Figure 5. Error diagrams from the point of view of the events (a) and alarms (b) identified by RST_{MWC} on the whole studied period (June 2005 to December 2015). In (a), the graph is zoomed to emphasize the achieved results. Empty triangles refer to the seismic events, within alerted volumes corresponding to $M_{JMA} \geq 6$ and 6.5, which occurred after or before SSTA appearances (preseismic and postseismic anomalies). Full triangles refer just to the events occurred after the SSTA appearances (only preseismic anomalies). Similarly, blue and red cross/plus symbols indicate the mean values of the results concerning the analyses performed by using different synthetic catalogs (see Table S1 in supporting information). Blue and red lines indicate the confidence limit curves surrounding the diagonal of random guess for earthquakes with $M_{JMA} \geq 6$ and 6.5, respectively. In this study, confidence levels of 95% are used to indicate the "significant" deviance from the random guessing function. In (b), full triangles refer to the SSTAs which are not followed by events with $M_{JMA} \geq 6$ and 6.5. Empty triangles refer to SSTAs not followed or preceded by seismic events. The dashed line indicates 95% confidence surrounding the random guess for the 29 identified SSTAs. For both diagrams, minimum and maximum probability gains (G) are reported. SSTA, Significant Sequence of Thermal Anomaly.

图5(a)显示，从事件的角度来看，警报已经被证明比随机猜测要好，但为了验证从警报的角度来看是否相同，我们建立了一个特设的错误图（图5(b)），考虑到

$$\nu_{\mathrm{SSTA}(M)} = \frac{\text{number of SSTAs not corresponding to EQs with magnitude} \geq M \left(\text{false positive}\right)}{\text{total number of SSTAs identified within the whole space} \times \text{time volume}} \tag{4}$$

$$\tau_{\mathrm{EQ}}\left(M\right) = \frac{\text{space} \times \text{time volume occupied by EQs with magnitude} \geq M}{\text{whole investigated space} \times \text{time volume}} \tag{5}$$

计算了震级≥M的地震所占据的时空域，其中：

- 时间窗口：从地震发生前30天到地震发生后15天（共46天）。
- 空间窗口： RD=10^0.43M，即Dobrovolsky半径（Dobrovolsky等人，1979）。

图5(b)强调，即使从报警的角度来看，SSTA也优于随机猜测。同样在这个测试中，概率增益被计算为G=（1-νSSTA）/τEQ。与随机猜测相比，获得的数值达到2.95（对于M≥6的地震之前的SSTA）。

作者还评估了地震群对所取得结果的可能影响（在Michael[1997]中也有讨论）。为了达到这个目的，我们保留了SSTA的空间特征和它们的时间长度，同时随机生成了每个SSTA的起始时间。通过这种方式，我们生成了50个合成SSTA的集合。图6(b)显示了Molchan分析的结果（只报告了在合成SSTA上取得的结果的平均值）。

这种分析的平均值（图6（b））和所有的结果（见辅助资料中的表S4）都落在误差图的不乐观区域；它们都在显著水平α=5%下拒绝了空假设。

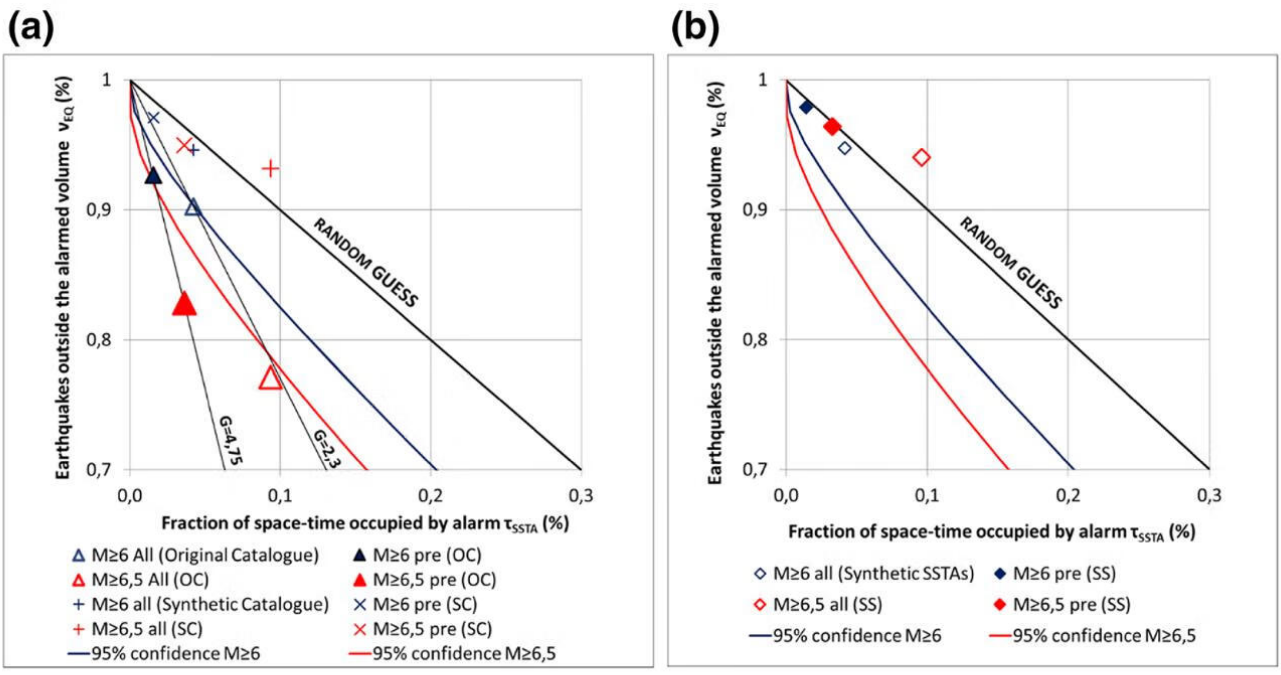

Figure 6. (a) Error diagram related to the analysis carried out with the earthquake catalog filtered on a monthly basis. As in Figure 5(a), results of the analyses performed by using synthetic catalogs (see Table S3 in supporting information) are also reported through their mean values. Symbol meaning is the same as in Figure 5(a). (b) Error diagram concerning the analysis carried out, taking random forecast (i.e., synthetic SSTAs) into account. The analysis has been performed considering as "target" the events belonging to the filtered monthly catalog. Blue and red rhombi indicate the mean values of results concerning the analyses performed by using synthetic SSTAs. Table S4 of the supporting information reports full details of the analysis. SSTAs, Significant Sequence of Thermal Anomalies.

3.多参数方法

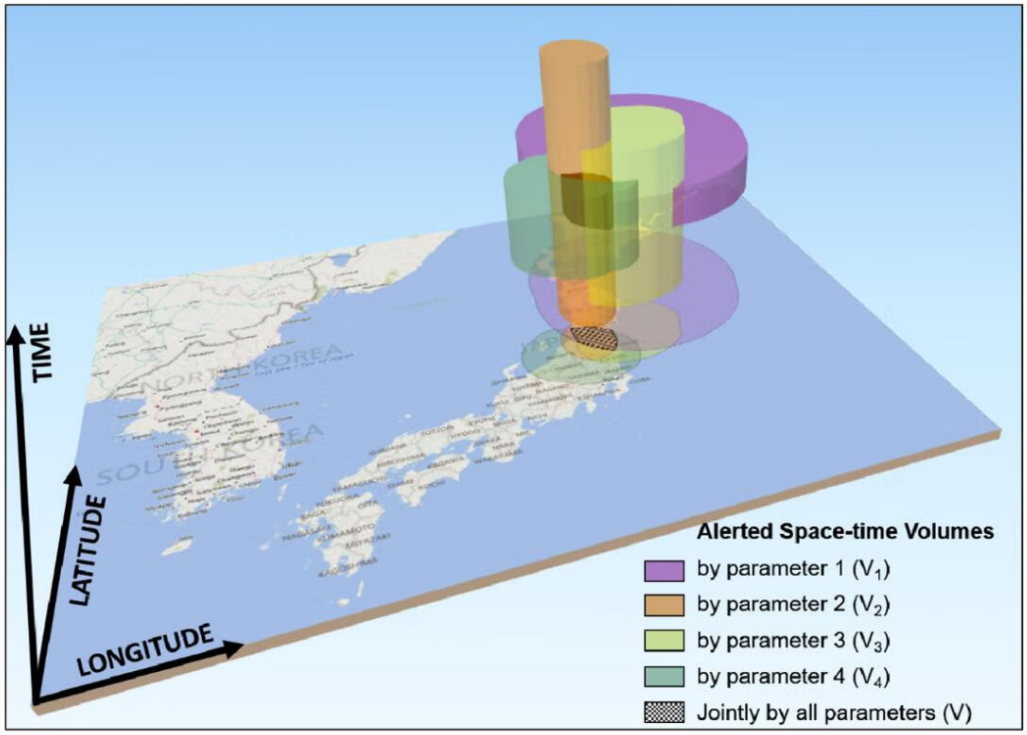

Figure 7. The schematic 3D representation of the reduction of the alerted space–time volume by a multiparametric approach. Colored cylinders represent the "alerted" space–time volumes V_i of each (nonseismological and seismological) parameter i. The intersection V of these cylinders identifies the jointly "alerted" space–time volume as a result of the integration of multiparametric observations.

4.扩展

4.1震前TIR异常提取主要研究和算法

Table 1 - Main studies and algorithms for pre-seismic TIR anomalies identification.

Methods	Authors	Satellite TIR sensors	Thermal Anomaly Definitions/ Indices	Reported Anomaly Intensities	Relation with EQ epicentre and time of occurrence		EQ Mag	Validation\ Confutation
					Affected area (km²)	Time-lag		
M1	Qiang *et al.*, 1991, 1992, 1997; Qiang and Dian, 1992	MFG/MVIRI	$\Delta T(x,y,t)=T(x,y,t)-\mu_1(t,H)$	2-10 K	100-50,000	3 days before	M 5.1 –7.0	V
M2	Huang and Luo, 1992	NOAA/ AVHRR	$\Delta T(x,y,t)=T(x,y,t)-\mu_1(t,A)$	----	----	----	----	C
M3	Tronin, 1996, 2000; Tronin *et al.*, 2002, 2004	NOAA/ AVHRR	$\Delta T(x,y,t)=T(x,y,t)-\mu_1(t,H)$	$\Delta T(x,y,t)>$ $2\text{-}\sigma_1(t,H)$	35,000	6-24 days before 7 days after	M 4.7 – 7.3	V
M4	Xu *et al.*, 2000	GMS	$\Delta T(x,y,t)=T(x,y,t)-\mu_1(t,H)$	>2 K	600,000	10 day before	M_S 7.6	V
M5	Lu *et al.*, 2000	NOAA/ AVHRR	$\Delta T(x,y,t) =$ $T(x,y,t) - T(x,y,t')$ with $t'<t$	8 K	40,000	1-2 days before	M_S 6.2	V
M6	Tramutoli *et al.*, 2001; Di Bello *et al.*, 2004;	NOAA/ AVHRR	$\otimes_{\Delta V}(x,y,m)=\mu_{\otimes}(x,y)$ $V(x,y,t)=T(x,y,t)$	$\otimes_{\Delta V}(x,y,m)>0,6$	100,000	3 days	$M_S=6.9$	V&C
			$V(x,y,t)=LST(x,y,t)$	$\otimes_{\Delta V}(x,y,m)>1$				
	Filizzola *et al.*, 2004; Corrado *et al.*, 2005; Tramutoli *et al.*, 2005; Aliano *et al.*, 2007, 2008a, 2008b; Genzano *et al.*, 2007, 2009a, 2009b, 2015; Lisi *et al.*, 2010, 2014; Pergola *et al.*, 2010; Eleftheriou *et al.*, 2015	NOAA/ AVHRR MFG/MVIRI GOES/ IMAGER MSG/SEVIRI EOS/ MODISGMS/ VISSR	$\otimes_{\Delta V}(x,y,t)=[\Delta V(x,y,t)-\mu_{DV}(x,y)]/$ $\sigma_{DV}(x,y)$ with $\Delta V(x,y,t)=V(x,y,t)-\mu_V(t)$ $V(x,y,t)=T(x,y,t)$ or $V(x,y,t)=LST(x,y,t)$	$\otimes(x,y,t)>1,5\div4$ (space/time persistence required)	100 -500,000	1-25 days before 1-5 days after	M_S 4.0 – 7.9	V&C
M7	Ouzounov and Freund, 2004	EOS/MODIS	$\Delta LST(t)=LST_{2002}(d)-LST_{2001}(d)$	4 K	30,000	1-10 days days before	M_S 7.9	V
	Ouzounov *et al.*, 2006	EOS/MODIS	$DLST(t_i)=LST_{RMS}(t_i)-LST_{RMS}$				M_S 6.8 – 7.9	
M8	Saraf and Choudhury, 2004, 2005a, 2005b, 2005c; Choudhury *et al.*, 2006; Rawat *et al.*, 2011; Saraf *et al.*, 2008, 2009, 2012	NOAA/ AVHRR	Visual Inspection	5-7 K	50,000-250,000	1-10 days before and 2-3 days after	M_W 5.8 – 7.7	V&C
M9	Yoshioka *et al.*, 2005	NOAA/ AVHRR	$\Delta T(x,y,t)=T(x,y,t)-\mu_1(t,D)$	4-8 K	50,000	2/3 days before	M_W 6.8	V&C
M10	Lixin *et al.*, 2006; Liu *et al.*, 2007	NOAA/ AVHRR	Visual Interpretation	4-5 K	80,000-920,000	1-25 days before and 2-3 days after	M_S 5.9	V
M11	Panda *et al.*, 2007	EOS/MODIS	$\Delta T(x,y,t)=T(x,y,t)-\mu_1(x,y,t)$	5-10 K	111,000	7 days before	M_W 7.6	V
M12	Halle *et al.*, 2008	NOAA/ AVHRR	As M6 with $V(x,y,t)=LST(x,y,t)$	$\otimes(x,y,t)>$ 2-3	2,600-5,000	2-10 days before and 4-7 days after	M =6.4-7.8	V&C
M13	Eneva *et al.*, 2008	EOS/MODIS	As M6 with $V(x,y,t)=LST(x,y,t)$ and with $\mu_{DV}(x,y)$ and $\sigma_{DV}(x,y)$ computed on 31 days before t	$\otimes(x,y,t)>2,5\div3,5$	----	20 days before - 20 days after	M 4.5 – 6.6	V&C
M14	Huang *et al.*, 2008	EOS/MODIS	Visual Inspection	3-5 K	----	1 day before	M_S 8.0	V

Methods	Authors	Satellite TIR sensors	Thermal Anomaly Definitions/ Indices	Reported Anomaly Intensities	Relation with EQ epicentre and time of occurrence		EQ Mag	Validation\ Confutation
					Affected area (km²)	Time-lag		
M15	Ouzounov *et al.*, 2006; Bleier *et al.*, 2009	EOS/MODIS GOES/ IMAGER	$T(x,y,t_i)=T_0+at_1$ (6pm<t_1<6am)	a > 0	- - - -	1-13 days before	M_w 7.7 M 5.4	V
M16	Piroddi, 2011; Piroddi and Ranieri, 2012; Piroddi *et al.*, 2014	MSG/SEVIRI	$<T(x,y,t_i)>=T_0+at_1$ (6pm<t_1<4am)		10,000	7 days before	M_w 6.3	V&C
M17	Chen *et al.*, 2010; Ma *et al.*, 2010; Saradjian and Akhoondzadeh, 2011	NOAA/ AVHRR EOS/MODIS	Wavelet transform	4-5 K	- - - -	15 days after	M >7.0	V
M18	Yang and Guo, 2010	MTSAT	$\Delta T_{year}(x,y,d)=[T_{year}(x,y,d)-T_{year-n}(x,y,d)]-T_{year}(x,y,d-1)$	4-5 K	30.000	1-14 days before	M_S 6.2	V
M19	Zhang *et al.*, 2010, 2011; Xie *et al.*, 2013	FY-2C FY-2E	Wavelet transform	4-10 K	10,000-600,000	Several days to 2 months before	M_S 7.2-9.0	V
M20	Saradjian and Akhoondzadeh, 2011	EOS/MODIS	interquartile, wavelet transform and Kalman filter method	1-4 K	- - - -	1-20 days before	M_w 6.1-6.6	V
M21	Zoran, 2012	EOS/MODIS	$\Delta LST(x,y,t)=(LST(x,y,t)-<LST>(t))/LST(x,y,t)$	10 K	30,000	15 days before	M_w 9.0	V
M22	Xiong *et al.*, 2013	AATSR	As M6 using $\otimes_{\Delta V}(x,y,t)=[\Delta V(x,y,t)-\mu_{DV}(x,y)]/\sigma_{DV}(x,y)$	$\otimes(x,y,t)>4$	130,000	15 days before	M_w 6.3	V&C

T(x,y,t) = TIR signal measured in correspondence of the geographical coordinates (x,y) at the time t
LST(x,y,t) = LST products computed in correspondence of the geographical coordinates (x,y) at the time t
mT(t,D) = spatial average over a seismically unperturbed zone (D) on the same image
mT(t,A) = spatial average over the same area (A) of punctual air temperature data (from meteorological stations and other sources).
mT(t,H) = spatial average over a selected restrict area (H) on the same image (*cloud-free, seismically unperturbed*)
$\otimes_{\Delta V}(x,y,m)=\mu_{\otimes}(x,y)$ = monthly average of daily RETIRA index $\otimes_{\Delta V}(x,y,t)$
$<T(x,y,t_i)>$= average of $T(x,y,t_i)$ on ten days before $LST_{RMS}(t_i)$ = the square root of the mean value of the quantity $LST^2(x,y,t_i)$ computed in an area of MxN km² (in the considered case 100x100 km²) centred on the epicentre

LSTRMS = temporal average computed on the precedent 60 or 90 days
$T(x,y,t) = T_0(x,y) + a(x,y).t$ is the linear regression function computed on the base of 41 MSG-SEVIRI TIR values (41, 15-min slots between 6 pm and 4 am) $T(x,y,t_i)$ corresponding to the averages on the previous 9 days where a(x,y) is the coefficient of the linear regression $<T(x,y,t)>$ is the average of $T(x,y,t_i)$ computed for each
$LST_y(d)$=spatial average of the LST(x,y,t) image collected night-time on the day d of the year y over an area of MxN km² (in the considered case 100x100 km²) centred on the epicentre
d= Julian day

MFG/MVIRI =Meteosat First Generation/Meteosat Visible and InfraRed Imager
NOAA/AVHRR = National Oceanic and Atmospheric Administration/Advanced Very High Resolution Radiometer
GMS = Geostationary Meteorological Satellite
GOES = Geostationary Operational Environmental Satellite/IMAGER

MSG/SEVIRI = Meteosat Second Generation/Spinning Enhanced Visible and Infrared Imager
EOS/MODIS= Earth Observing System/Moderate Resolution Imaging Spectroradiometer
MTSAT= Multifunctional Transport Satellites
FY-2C= Fengyan 2C


南
北
想你的风还是吹到了雁栖湖
S
WELCOME TO 雁水路3号
N